A Current Regulated Pulse Width Modulation Method with New Series Resonant Inverter

Sun-Soon Park and Gyu-Hyeong Cho

Department of Electrical Engineering
Korea Advanced Institute of Science and Technology
P.O. Box 150, Chongryang, Seoul, 131-650, Korea

Abstract

In this paper, a new series resonant inverter which can be constructed simply using natural commutation switches is proposed. The proposed inverter can be operated on full four quadrant with almost unity power factor. It is also shown that the proposed inverter does not require damping circuit or special control loop for stabilization and solved the inherent problem in series resonant inverter such as oscillation. Simulation results also show that the output current is well regulated to the command value without scarificing the advantages.

Introduction

Generally, typical schemes of resonant converters(or inverter) can be classified into series resonant and parallel resonant schemes and the utility of both schemes are well documented in many references[1]-[5]. The ac resonant circuit, however, impresses both polarities of ac voltage and current on the link and thus the switches should be bidirectional. These switches are usually realized by two inverse-parallel transistor or thyristors for the parallel or series resonant circuit.

The dc-link circuits of Fig.1 realize pulsating dc currents in the link by adding dc offset to the ac resonant currcnt[6]. This series resonant dc-link scheme can be implemented with simple configuration having unidirectional switches. In this case, switching action of the converters occurs at the zero crossing instants of the link current. Since the link current is unidirectional, usual six thyristors are needed per converter bridge.

On the other hand, because the filter capacitance C is required at the output side for the resonant converter in this series resonant dc-link scheme, a high frequency parasitic oscillation is inevitable in the inverter output. This oscillation is caused by interactions between the filter capacitance C and the load inductance L including the series resonant dc-link L_o, C_o. Even if the system is accurately controlled, the parasitic oscillation remains almost independent of the load current[6].

Stabilization is, however, accomplished by derivative feedback as shown in Fig, 2. The stability of the system is improved comparing with the case of no derivative feedback but it still has a parasitic oscillation. In order to reduce further or absorb the high frequency component caused by the current pulses, the damper circuit shown in Fig. 3 is found to be effective. Although the parasitic oscillation is reduced by the feedback damping circuit, the system has shortcomings such as noise problem due to the derivative feedback, increased complexity of the power circuit,etc. One of the demerits is that the system efficiency is reduced due to the damping circuit.

In this paper, a new method is suggested to eliminate the oscillation problem without using the derivative feedback and the damping circuit. The proposed scheme can be constructed with the unidirectional and natural commutation switches having a simple small size inductor on the dc link side instead of resonant link. The switchings of the converters occur at the zero crossing instants of the link current like the series resonant dc-link scheme. This scheme is operable well on full four-quadrants and controllable to have almost unity power factor since the converter only operats on

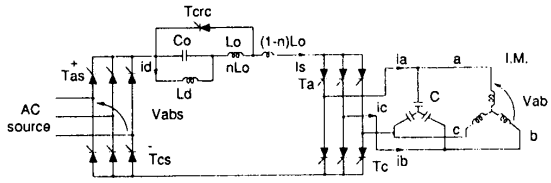

Fig. 1 The series resonant dc-link scheme

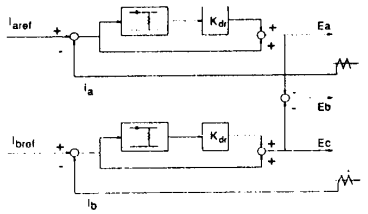

Fig. 2 Derivative feedback loop for stabilization of Fig. 1

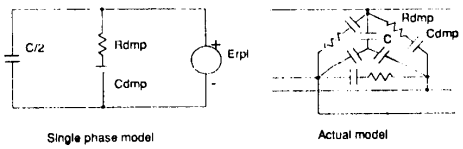

Fig. 3 Damper circuit for absorbing the high frequency current pulses in Fig. 1.

one of three modes composed of rectifying, regenerating and freewheeling modes. The advantages of the proposed scheme are shown through analyses and simulation results.

Descriptions of The Proposed Inverter

The power circuit of the proposed scheme can be realized with unidirectional and natural commutation switches as shown in Fig.4. The power circuit looks the same as that of the conventional current source inverter(not resonant) having the output side capacitor filter[7]. The proposed scheme, however, is very different from the conventional CSI in the sense of the parameter size and operations. The proposed scheme is unique in the operation characteristics.

The current regulation method in this scheme is similar to the conventional current regulated pulse-width modulation(CRPWM). In the CRPWM, the source voltage which is switched according to the hysteresis current control rule is applied to the stator of the induction motor. The source voltage in the conventional CRPWM corresponds to the command voltage in the new proposed scheme. According to this command voltage, the stator voltage is regulated through the inverter switching, which is illustrated in the next sec-

89CH2792-0/89/0000-1045$01.00 © 1989 IEEE

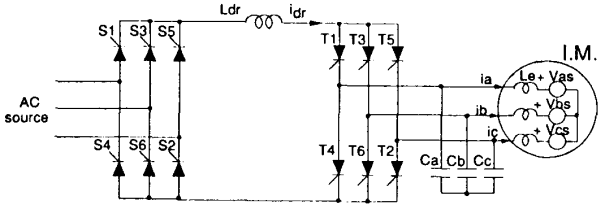

Fig. 4 New partial series resonant inverter for three phase load.

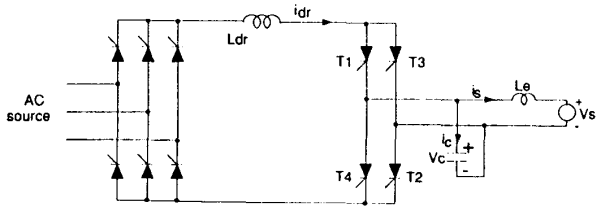

Fig. 5 Single phase configration of the proposed scheme

tions. On the other hand, the resonant inductance L_{dr} and the capacitances C_c forms the series resonant circuit, however, this circuit is partially resonant rather than fully resonant in the view point of the capacitance C_c. The purpose of resonance is used for the switch commutations and the capacitor voltage swings near the full rectifying voltage while the inductance current resonants from zero to full current for every half cycle. Therefore, the converter operates in almost unity powerfactor.

Operation Principle for The Single Phase Configuration

Before describing the three phase inverter, a single phase inverter is illustrated due to its simplicity to show the proposed idea clearly. Fig. 5 shows the proposed inverter which is implemented with the thyristors. The power circuit looks the same to the conventional CSI with output filter in appearance, however, its operation principle is completely different and the inductance and capacitance sizes are very small compared with those of the conventional CSI. The uniqueness of this scheme is shown through the mode analyses.

I) Powering Mode

It is assumed that the load side capacitor have been initially charged with initial voltage V_{co}^{+} or V_{co}^{-} and its value is determined by

$$V_{co}^{+} = V_r - \Delta V \qquad \text{for } i_s > 0$$

$$V_{co}^{-} = V_r + \Delta V \qquad \text{for } i_s < 0 \qquad (1)$$

where V_r is the maximum rectified voltage of the converter side and ΔV is initially chosen arbitrary with any value.

Powering mode(mode I) starts with thyristors T_1 and T_2 turned on while the source side converter operate on its maximum value. The resonant link current i_{dr} flowing through L_{dr} and T_1 due to the difference of V_{dc} and V_{co} begins to charge the resonant capacitorC_c. In this mode, the simplified equivalent circuit is shown in Fig. 6-(a) and the resonant link current i_{dr}, the capacitor voltage v_c and the capacitor current i_c are shown in Fig. 6-(c), respectively, in the steady state.

The resonant inductor current, the capacitor voltage and the capacitor current in this mode are given by ;

$$i_{dr}(t) = \frac{\Delta V}{Z_d} \sin(\omega_d t) + i_s(1-\cos(\omega_d t)) \qquad (2)$$

$$v_{cr}(t) = V_r - \Delta V \cos(\omega_d t) - Z_d i_s \sin(\omega_d t) \qquad (3)$$

$$i_c(t) = i_{dr} - i_s \qquad (4)$$

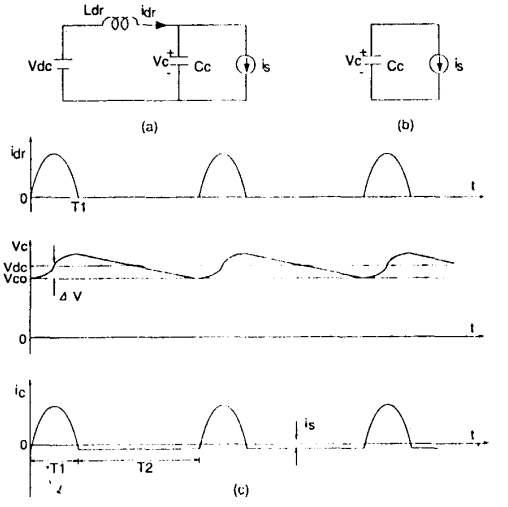

Fig. 6 Simplified equivalent circuit and waveforms : (a)Powing mode, (b)Discharging mode, (c)voltage and current waveforms.

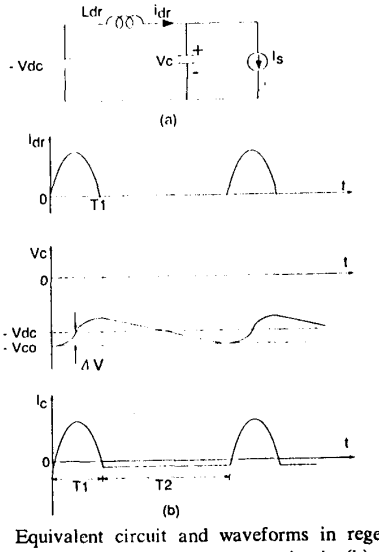

Fig. 7 Equivalent circuit and waveforms in regenerating mode, (a)simplified equivalent circuit, (b)capacitor voltage and capacitor current waveforms.

where $\Delta V = V_r - V_{co}$, $\omega_d = \frac{1}{\sqrt{L_{dr}C_c}}$ and $Z_d = \sqrt{\frac{L_{dr}}{C_c}}$.

After a finite period of time T_1, the powering mode is terminated when the resonance inductor current i_{dr} reaches zero. The interval T_1 is determined both by the resonant circuit parameters and by the load current. The interval length can be roughly estimated by

$$T_1 \cong \frac{\pi}{\omega_d} \quad . \qquad (5)$$

II) Discharging/charging mode

At the end of mode I, the switches are turned-off due to zero current in the switches, and the current loop only remains as shown Fig-6 (b). In this mode, the capacitor is almost linearly discharged because the load inductance are much larger than that of the

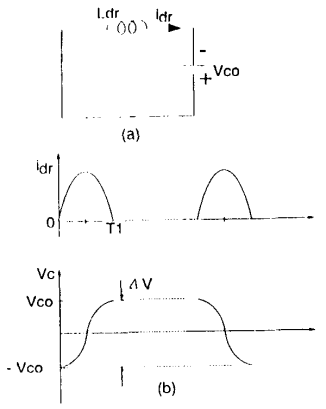

Fig. 8 (a)Equivalent circuit and waveforms in state changing mode, (b)inductor current and capacitor voltage waveforms.

resonant inductance L_{dr} and the load current is almost kept constant during this short interval. This mode continues until the capacitor voltage v_c reachs around the initial voltage V_{co} of mode I. Then the length T_2 is almost determined by the load condition and approximately expressed by

$$T_2 \cong \frac{2\Delta V}{I_s} C_c \quad . \tag{6}$$

III) Regenerative Mode

If it is again assumed that the resonant capacitor initially charged with V_{co}^+ or V_{co}^-, its value is also given by

$$V_{co}^+ = -V_r - \Delta V \qquad \text{for } i_s > 0$$
$$V_{co}^- = -V_r + \Delta V \qquad \text{for } i_s < 0 \quad . \tag{7}$$

From this condition, the simplified equivalent circuit can be drawn as Fig. 7-(a) when the thyristors T_1 and T_2 turned on. The waveforms of the inductor current, capacitor voltage and capacitor current are shown in Fig. 7-(b). Assuming that the load current is almost kept constant and the converter is operated on fully regenerating mode (or firing angle $\alpha = 180^o$), then the inductor current and the capacitor voltage are analytically expressed as:

$$i_{dr}(t) = \frac{\Delta V}{Z_d} sin(\omega_d t) + i_s(1-cos(\omega_d t)) \quad . \tag{8}$$

$$v_{cr}(t) = -V_r - \Delta V cos(\omega_d t) - Z_d i_s sin(\omega_d t) \tag{9}$$

At the end of the mode, the circuit operates on the dissipative mode (mode II) similar to the end of the mode I.

IV) State Changing Mode

When the powering mode is switched to the regenerative mode, or vice versa, the capacitor voltage must be reversed to its opposite polarity. This action can be obtained by operating the converter on the free reversing state as shown in Fig. 8. Fig. 8-(b) shows resonant link inductor current and capacitor voltage, respectively, in this mode and these current and voltage waveforms are expressed as:

$$i_{dr}(t) = \frac{V_{co}}{Z_d} sin(\omega_d t) + i_s(1-cos(\omega_d t)) \tag{10}$$

$$v_c(t) = -V_{co} cos(\omega_d t) - Z_d i_s sin(\omega_d t) \quad . \tag{11}$$

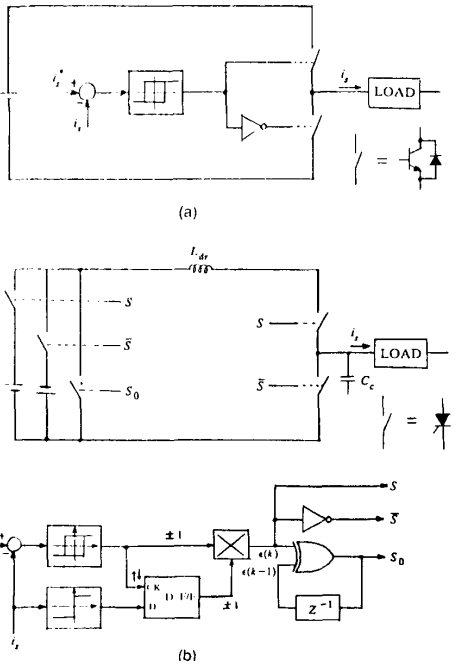

Fig. 9 Current regulation scheme : (a)the conventional CRPWM method, (b)the proposed current regulation method.

Comparison of Constant ΔV and Constant Pulse Density Operation

The method in the previous illustrations is again classfied with two method. One method which constantly control the ΔV propery turned on the thyristors whenever the capacitor voltage become the $V_c^* + \Delta V$. In this case, the peak current of resonant-link inductance is not depend on load condition, and so maintained with almost constant. On the other hand, the costant pulse density operation is periodically turn-on the thyristors. The ΔV and the peak current of resonant-link inductance are propertional to the load current.

Two methods can be used for current regulation, however, the constant pulse density method is more profitable because the constant ΔV method require the capacitor voltage sensing, and then, the control logic is more complexible. In the constant ΔV operation, the ratio of the peak current of link inductance and average load current are very large in small load current range. However, the constant pulse density method not require the capacitor voltage sensing and the peak current of link inductance is automatically controlled according to the load condition. Becase of these reasons, the constant puse density operation have more advantages for the load current regulation.

Current Regulation Method

The current regulation method used in this series resonant inverter is very similar to the conventional CRPWM method except that the system can be constructed with thyristors and be operatable on regenerating mode. In the process of current regulation, Fig. 9 shows the similarity and the difference between the conventional CRPWM and the proposed current regulation method.

Fig. 10-(a) and (b) show the current command i_s^*, actual current i_s and the command voltage v_s^*. In the proposed system, the voltage regulation process is added to the current regulation

Table 1. Mode selection and operation in each state

current error	current	selacted mode	starting condition	turn-on thyristors	converter output	mode II operation
$\epsilon_i > 0$	$i_a > 0$	I	$V_c < V_{dc} - \Delta V$	T_1, T_2	V_{dc}	discharging
	$i_a < 0$	III	$V_c > V_{dc} + \Delta V$	T_3, T_4	$-V_{dc}$	charging
$\epsilon_i < 0$	$i_a > 0$	III	$V_c < -V_{dc} - \Delta V$	T_3, T_4	$-V_{dc}$	discharging
	$i_a < 0$	I	$V_c > -V_{dc} + \Delta V$	T_1, T_2	V_{dc}	charging

because the natural commutation switches are used instead of the forced commutation switches different from the conventional CRPWM. The process how the output voltage is regulated according to the command value, and the process how the output current is regulated can be easily understandable by examing the Table 1 and Fig. 10 (c)-(e). In negative load current condition, however, the switching condition and the operation mode are slightly different comparing with the positive load current condition. Fig.11 shows the process of the current regulation and the operation modes and the switching conditions are also shown as table 1 when the load current is negative.

Three Phase Configuration of The Proposed Method

Three phase configuration of the proposed method as shown in Fig. 4 can also be operated with natural commutation switches. The operating principle of the three phase type is very similar to the single phase type as described previously. However, the three phase inverter is more complicated comparing with the single phase one because each phase is dependent on the other phases.

The control rule in this inverter is to faithfully follow up the conventional CRPWM method as possible. The voltage command is obtained from the current error as the conventional CRPWM. In the proposed method, however, the converter output voltage also be controlled depending on the inverter output current direction because the inverter and converter switches are unidirectional. In more detail, if the polarities of the current and its error are the same, the converter output voltage is controlled refering to the maximum phase current, but if the polarities are opposite, it is controlled refering to the minimum (or absolute maximum in negative polarity) phase current so that the current direction is satisfied since the switches are unidirectional.

In this system, the control rule is given in sequence as follows. Firstly, the most significant phase(MSP) whose polarity of the current error is different from the two other phases must be determined. The MSP can be logically obtained by

$$\begin{aligned} MSP_A &= S_{\epsilon_B} S_{\epsilon_C} + \overline{S}_{\epsilon_B} \overline{S}_{\epsilon_C} \\ MSP_B &= S_{\epsilon_C} S_{\epsilon_A} + \overline{S}_{\epsilon_C} \overline{S}_{\epsilon_A} \\ MSP_C &= S_{\epsilon_A} S_{\epsilon_B} + \overline{S}_{\epsilon_A} \overline{S}_{\epsilon_B} \end{aligned} \tag{12}$$

where S_{ϵ_A} is the sign of the error between the command and the actual value in A-phase current.

Next significant phase is obtained according to the direction of MSP and the remaining phase current, in other words, the phase which is opposit to a direction of MSP current is determined as the next significant phase (NSP). If A-phase is MSP, NSP is also logically determined as

$$\begin{aligned} NSP_B &= S_{i_A} \oplus S_{i_B} \\ NSP_C &= S_{i_A} \oplus S_{i_C} \end{aligned} \tag{13}$$

where S_{i_A} is the sign of the A-phase current and the notation '$\oplus$', means the exclusive-OR operation. By doing so, two phases can be determinded with NSP in accordance with the current state. Two NSP's(or one NSP and the remaining phase) form parallel connection of the capacitor voltages. The MSP-leg is connected to the positive side of the link when the polarity of the MSP current is positive whereas NSP-leg is contected to the negative side. When the MSP current is negative, however, it is connected reversely as shown in the above illustration. On other hand, the converter output voltage is logically determined by

$$\begin{aligned} V_{dc} &= V_r \quad : \textit{in same polarity of MSP current and itserror} \\ V_{dc} &= -V_r \quad : \textit{in opposite polarity of MSP current and its error} \end{aligned} \tag{14}$$

In conclusion, the mode selection for all states of the currents and their errors are shown in the table of Appendix A. The structure can be classified into four types as shown in Fig. 12. The analysis of the structures are presented in Appendix B.

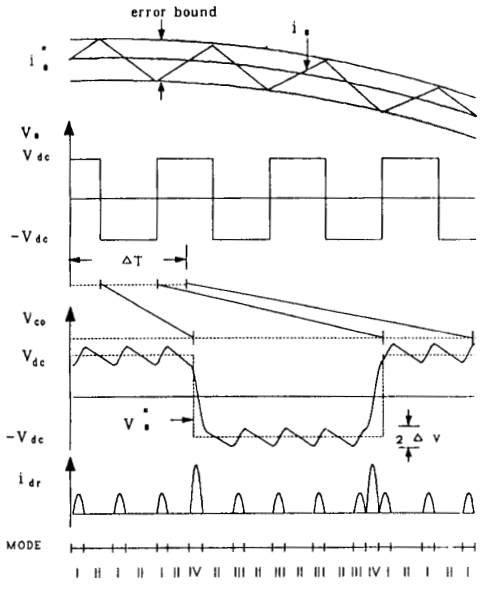

Fig. 10 Control algorithm of current regulation in positive load current.

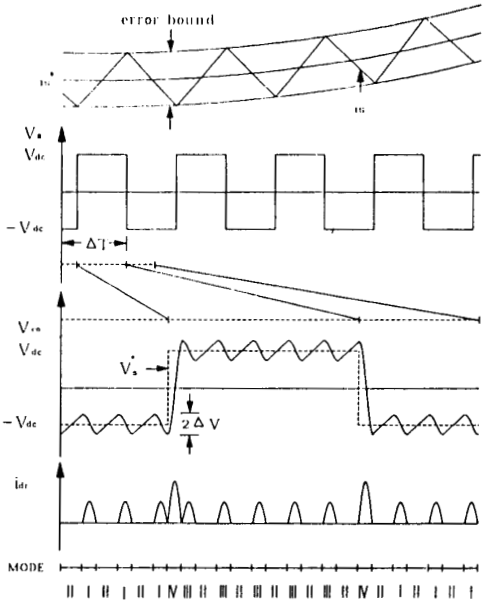

Fig. 11 Control algorithm of current regulation in negative load current.

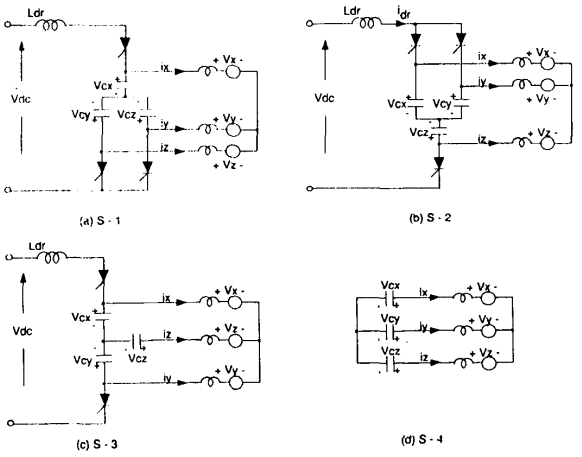

Fig. 12 Three phase switching structures.

Operation Modes

The operation of the three phase configuration also has four modes : powering mode, discharging/charging mode, regenerating mode and balancing mode. The MSP in the three phase type is matched to the single phase type and the mode selection is fully determined by the condition of MSP. The mode selection strateges corresponding to each condition are shown in appendix A.

i) MODE I : Powering mode

If the MSP is determined to C-phase and the NSPs are determinded to both A and B-phases, the simplified equivalent circuit on powering mode (MODE I) operation, is shown in Fig. 13. In Fig. 13-(b), V_s^* is a command voltage for current regulation. This figure illustrates that the difference of V_{c_a} and V_{c_b} is equalized around the command voltage V_s^*. The dc-link inductor current i_{dr} is shown in Fig. 13-(c). In this mode, the points P_1 and P_2 at voltage and current waveforms, respectively, show the boundary of the different resonant frequency because of the difference of resonant capacitances C_a and $C_a + C_b$, respectively. In other words, turning-on of one thyristor (T_3) is delayed to the other(T_1 in this case).

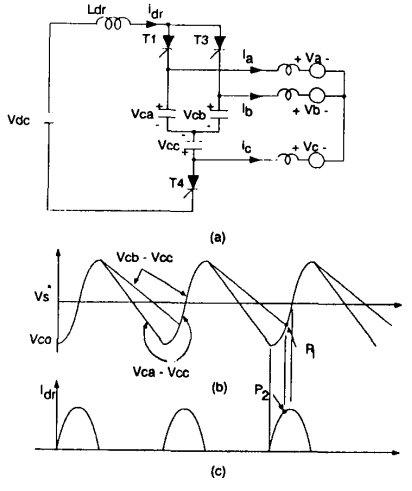

Fig. 13 An illustration of powring mode operation under the conditions of $\epsilon_a > 0$, $\epsilon_b > 0$ and $\epsilon_c < 0$ for $i_a > 0$, $i_b < 0$, $i_c < 0$ and $i_a > i_b$.

ii) MODE II : Discharging/charging mode

At the end of mode I, the discharging mode (Mode II) which is isolated from the inverter input link starts and the capacitors are simply charged or dischargrd by the load current. This process continues untill the powering mode restarts. In other words, $V_{C_{ab}}$ is discharged to $V_{dc} - \Delta V$ as shown in Fig. 13.

iii) MODE III : Regenerating mode

The regerating mode(MODE III) is formed under the condition that the polarities between the current and the current error in MSP are not equal. The operation of the regenerating mode is very similar to the powering mode except that the capacitor voltage and V_{dc} are reversed each other.

iv) MODE IV : Balancing mode

When the NSP's are fortunately determined to two-phases, in other words the polarities of NSP's currents are same, the voltages of two NSP's parallel capacitors in powering or regenerating mode are naturally balanced. Note that they are unbalanced in dissipative mode when the current polarities of two phase except on MSP's are opposite and then NSP is only one. In other words, the vlotage balancing of the parallel capacitors dose not occur in nature. For an example, when $\epsilon_a > 0, \epsilon_b > 0$ and $\epsilon_c < 0$ in current error and $i_a > 0$, $i_b < 0$, $i_c < 0$, the MSP is C-phase and the current polarities A-phase and B-phase are opposite. In this case, the NSP is A-phase and C_a is discharged in mode II whereas the C_b is charged. Therefore,if the balancing mode have no in mode II, the capacitor voltage of B-phase is contineously increased.

The balansing operation is performed through difference of two capacitor voltage except on MSP's reversing by freewheeling as shown in Fig. 14. At the end of the balancing mode, the two parallel capacitor voltages are exchanged each other such as show in Fig. 14-(c). And then, the difference of two capacitor voltages can always be bounded to some value less then $2\Delta V$.

v) MODE V : State changing mode

When the sign of the capacitor voltages have opposite to the sign of the command value, the capacitor voltages mst be reversed by freewheeling action through the converter and resonant-link inductance like single phase operation. Therefore, the capacitor voltage be matained to the wanted value for current regulation.

Simulation Results

Simulation is performed for three phase case when the parameter value are $L_e = 4.1\ mH$, $R_s = 0.56\ \Omega$, $C_c = 1.0\ \mu F$, $L_{dr} = 50\ \mu H$, $\omega_d = 2\pi \cdot 22{,}000\ rad/sec$. Fig.15 shows the simulation results when the induction motor operates on motoring region

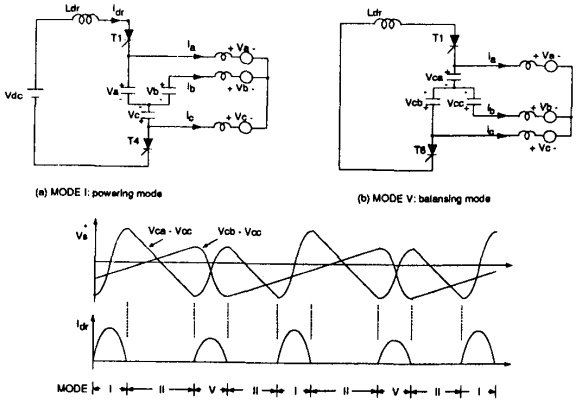

Fig. 14 Powering and balansing mode operations under the condition of $\epsilon_a > 0$, $\epsilon_b > 0$ and $\epsilon_c < 0$ when $i_a > 0$, $i_b < 0$, and $i_c < 0$.

at $60H_z$. In this case, the error baundary of the current hysteresis control is fixed to $+0.5A$. Fig.15-(a) shows that the stator current is well regulated within the given error baundary while the stator voltage $V_{C_{ab}}$ (or two capacitor voltage difference) swings between $V_{dc} - \Delta V$ and $V_{dc} + \Delta V$ as shown in Fig. 15-(c). The capacitor voltage V_C and the inductor current i_{dr} are also shown in Fig.15-(b) and (d). Fig.16 are the waveforms showing that the induction motor operates on the regenerating region as the same condition shown in Fig.15. The performance of the regenerative operation is thought to be good enough like motoring operation.

Fig. 17 shows a transient response for abrupt command change from 5 A to 10 A. In this case, the current response is quick and well regulated to the command value. Fig. 18 shows that current is also regulated well even when the frequency command is quickly changed. The simulation results show that the current regulation of the proposed scheme is good enough not only in the steady state but also in transient. This scheme also shows that the parasitic oscillation does not occur without using even the damping circuits and the stabilized control loops.

Conclusion

A new partial series resonant inverter having a simple configuration is proposed. It is shown that the proposed inverter can be implemented with all natural commutation switches. It is also shown that the inherent problem such as paracitic oscillation can be eliminated without using damping circuits or special control loops for stabilization. The proposed inverter can operate on the regenerating mode as well as on the powering mode with always unity power factor. Several features are shown through the simulation results. One demerit is the complexity of the control circuit, however, the proposed inverter could be excellently chosen for drive applications because of its numerous merits.

References

[1] P. Sood and T. A Lipo, "Power Conversion Distribution System Using a Resonant High-Frequency AC Link," *IEEE-IAS Annual Meeting Conference Record, pp 533-541* , 1986.

[2] H. K. Lauw, J.B. Klaassens, N. G. Butler and D. B. Seely, "Variable-Speed Generation with the Series Resonant Converter," *IEEE-PES Winter Meeting Conference Record* , 1987/1988.

[3] S. W. H. de Hann and J. D. Lodder, "A Formalistic Approach to Series-Resonant Power Conversion," *ESE Conference Record, pp. 231-238* , 1987.

[4] D. M. Divan, "The Resonant DC Link Converter--A New Concept in Static Power Conversion," *IEEE-IAS Annual Meeting Conference Record, pp.648-656* , 1986.

[5] D. M. Divan and G. L. Skibinski, "Zero Switching Loss Inverters for High Power Application," *IEEE-IAS Annual Meeting Conference Record, pp.627-634* , 1987.

[6] Y. Murai and T. A. Lipo, "High Frequency Series Resonant DC Link Power Conversion," *IEEE-IAS Annual Meeting Conference Record, pp.772-779* , 1988.

[7] Mitsuyuki Honibu, Shigeta Ueda and Akiteru Ueda, "A Current Souce GTO Inverter with Sinusoidal Inputs and Outputs," *IEEE Trans. Ind. Appl., vol. IA-23, NO.2, pp. 247-255* , March/April 1987.

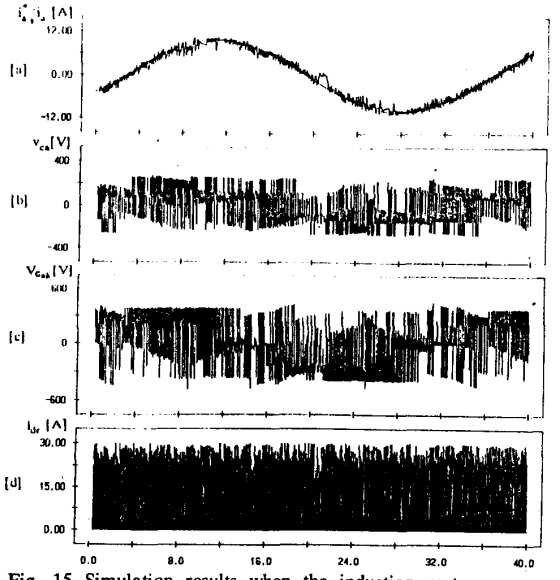

Fig. 15 Simulation results when the induction motor runs at 60 Hz motoring region : (a)command and actual currents, (b)capacitor voltage v_{c_a}, (c)line-to-line voltage $v_{c_a} - v_{c_b}$ and (d)resonant inductor current i_{dr}.

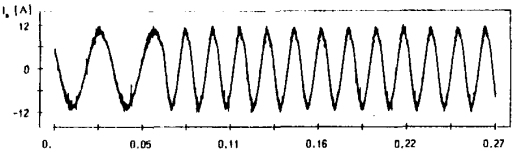

Fig. 17 Current waveforms when the magnitude of the current command is abruptly changed between 5 A and 10 A.

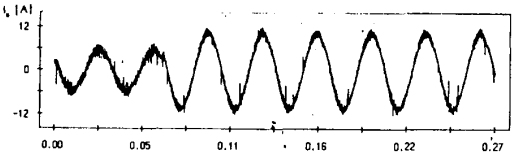

Fig. 18 Current waveforms when the frequency of the current command is abruptly changed between 30 Hz and 60 Hz.

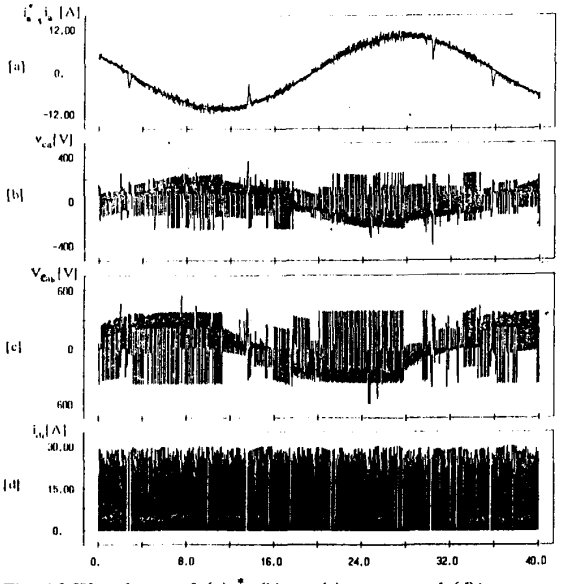

Fig. 16 Waveforms of (a)i_a^*, (b)v_{c_a}, (c)$v_{c_a} - v_{c_b}$ and (d)i_{dr} in regenerative region.

Appendix A

Table A-1 Most significant phases(MSP).

current error polarity			MSP
A	B	C	
-	-	+	C
-	+	-	B
-	+	+	A
+	-	-	A
+	-	+	B
+	+	-	C

Table A-2 Control of source side converter output voltage V_{dc}.

Error polarity in MSP	Current polarity in MSP	V_{dc}
-	-	V_f
-	+	$-V_r$
+	-	$-V_r$
+	+	V_f

Table A-3 Thyristors in conduction and corresponding strutures for every state.

MSP	Current polarity			NSP	Turn-on Structure	Thyristors
	A	B	C			
A-phase	-	-	+	C	S-3	T_4, T_5
	-	+	-	B	S-3	T_4, T_3
	-	+	+	B,C	S-2	T_4, T_5, T_3
	+	-	-	B,C	S-1	T_1, T_6, T_2
	+	-	+	B	S-3	T_1, T_6
	+	+	-	C	S-3	T_1, T_2
B-phase	-	-	+	C	S-3	T_2, T_3
	-	+	-	A,C	S-1	T_1, T_5, T_6
	-	+	+	A	S-3	T_3, T_4
	+	-	-	A	S-3	T_1, T_6
	+	-	+	A,C	S-2	T_2, T_3, T_4
	+	+	-	C	S-3	T_5, T_6
C-phase	-	-	+	A,B	S-1	T_4, T_5, T_6
	-	+	-	B	S-3	T_2, T_3
	-	+	+	A	S-3	T_4, T_5
	+	-	-	A	S-3	T_1, T_2
	+	-	+	B	S-3	T_5, T_6
	+	+	-	A,B	S-2	T_1, T_2, T_3

Appendix B

B. Analysis for three phase load

B-1. Derivative equations

$$\frac{di_{dr}}{dt} = (V_{dr} - V_l)/L_{dr} = \Delta V/L_{dr}$$

$$\frac{dV_{C_x}}{dt} = (i_{inx} - i_x)/C_c$$

$$\frac{dV_{C_y}}{dt} = (i_{iny} - i_y)/C_c$$

$$\frac{dV_{C_z}}{dt} = (i_{inz} - i_z)/C_c$$

B-2. Solution of the equations in B-1

$$i_{dr} = \frac{\Delta V}{Z_d}\sin(\omega_d t) + \frac{1}{2} I_s(1-\cos\omega_d t)$$

$$V_{C_x} = V_{C_x}(0) + \frac{1}{2}\Delta V_x(1-\cos\omega_d t) + \frac{1}{4} Z_d i_{s1}\sin\omega_d t + i_{o_1} t/C_c$$

$$V_{C_y} = V_{C_y}(0) + \frac{1}{2}\Delta V_y(1-\cos\omega_d t) + \frac{1}{4} Z_d i_{s2}\sin\omega_d t + i_{o_2} t/C_c$$

$$V_{C_z} = V_{C_z}(0) + \frac{1}{2}\Delta V_z(1-\cos\omega_d t) + \frac{1}{4} Z_d i_{s3}\sin\omega_d t + i_{o_3} t/C_c$$

Table B-1 Changing variables in the equations of appendix B.

variable change	structure-1		
	$V_{C_y} > V_{C_z}$	$V_{C_y} < V_{C_z}$	$V_{C_y} = V_{C_z}$
V_l	$V_{C_x} - V_{C_y}$	$V_{C_x} - V_{C_z}$	$V_{C_x} - V_{C_y}$
i_{inx} , i_{iny} , i_{inz}	i_{dr} , $-i_{dr}$, 0	i_{dr} , 0 , $-i_{dr}$	i_{dr} , $-1/2i_{dr}$, $-1/2i_{dr}$
i_{o_1} , i_{o_2} , i_{o_3}	$1/2i_z$, $1/2i_z$, $-i_z$	$1/2i_y$, $-i_z$, $1/2i_z$	0 ,0 , 0
I_s	$i_z - i_y$	$i_x - i_z$	$2i_x$
i_{s_1} , i_{s_2} , i_{s_3}	I_x , I_x , 0	I_x , 0 ,I_x	i_x , i_y , i_z
ΔV_x , ΔV_y , ΔV_z	ΔV , $-\Delta V$, 0	ΔV , 0 , $-\Delta V$	$2/3\Delta V$, $-1/3\Delta V$, $-1/3\Delta V$

structure-2			structure-3
$V_{C_x} > V_{C_y}$	$V_{C_x} < V_{C_y}$	$V_{C_x} = V_{C_y}$	
$V_{C_x} - V_{C_z}$	$V_{C_y} - V_{C_z}$	$V_{C_x} - V_{C_z}$	$V_{C_x} - V_{C_y}$
i_{dr} , 0 , $-i_{dr}$	0 , i_{dr} , $-i_{dr}$	$1/2i_{dr}$, $1/2i_{dr}$, $-i_{dr}$	i_{dr} , $-i_{dr}$, 0
$1/2i_y$, i_y , $1/2i_y$	$-i_x$, $1/2i_x$, $1/2i_x$	0 ,0 , 0	$1/2i_x$, $1/2i_x$, $-i_x$
$i_x - i_z$	$i_y - i_x$	$-2i_z$	$i_x - i_y$
I_x , 0 ,I_x	0 , I_x , I_x	i_x , i_y , i_z	I_x , I_x , 0
ΔV , 0 , $-\Delta V$	0 , ΔV , $-\Delta V$	$1/3\Delta V$, $1/3\Delta V$, $-2/3\Delta V$	ΔV , $-\Delta V$, 0